European Polymer Journal 78 (2016) 14–24

Contents lists available at ScienceDirect

European Polymer Journal

journal homepage: www.elsevier.com/locate/europolj

Macromolecular Nanotechnology

Responsive nanogels for application as smart carriers in endocytic pH-triggered drug delivery systems

Julio César Cuggino [a,1], Maria Molina [b,1], Stefanie Wedepohl [b], Cecilia Inés Alvarez Igarzabal [c], Marcelo Calderón [b], Luis Marcelino Gugliotta [a,*]

[a] Instituto de Desarrollo Tecnológico para la Industria Química (INTEC), CONICET, Güemes 3450, Santa Fe 3000, Argentina
[b] Institut für Chemie und Biochemie, Freie Universität Berlin, Takustrasse 3, Berlin 14195, Germany
[c] Departamento de Química Orgánica, Facultad de Ciencias Químicas, Universidad Nacional de Córdoba (UNC), IMBIV-CONICET, Haya de la Torre y Medina Allende, Ciudad Universitaria, Córdoba 5000, Argentina

ARTICLE INFO

Article history:
Received 30 October 2015
Received in revised form 11 February 2016
Accepted 23 February 2016
Available online 24 February 2016

Keywords:
Cancer
Doxorubicin
Drug delivery
Ionic complexes
Nanogels
Nanomedicine
NIPA-co-AAc
pH triggered

ABSTRACT

Various specially designed poly(N-isopropylacrylamide-co-acrylic acid) (NIPA-co-AAc) nanogels (NGs) with different NIPA/AAc molar composition were synthesized by precipitation/dispersion polymerization and evaluated as carriers for drug delivery systems (DDSs) of doxorubicin hydrochloride (DOXO·HCl) for cancer therapies. The NGs presented excellent dispersability in physiological environments (pH 7.4 and 5 at 37 °C), as shown by dynamic light scattering (DLS). Moreover, the NGs exhibited high drug loading capacity and efficiency due to the ionic interaction of the cationic drug with the anionic NGs. NG-DOXO·HCl formulation presented excellent dispersability in water and minimal leakage of the cargo at plasma simulated medium (pH 7.4 and 0.14 M NaCl) at 37 °C and a triggered release at lysosomal simulated medium (pH 5 and 0.14 M NaCl). This release behavior together with their size and the low cytotoxicity determined by the MTT assay converts these NGs in great candidates for their application as carriers in cancer therapies based on the enhanced permeability and retention effect (EPR) with drug pH-triggered release after endocytosis in tumor cells.

1. Introduction

The design of nanomaterials for their utilization as carriers in drug delivery systems (DDSs) of pharmaceuticals is an area of tremendous interest for academics and industrial research in the last years [1–6]. Especially for cancer therapies, where very toxic drugs are employed, the development of new nanocarriers that can transport the drug specifically to the action site (tumor), release the drug only there, and reduce the side effects after drug administration is of vital relevance [7,8]. Doxorubicin (DOXO) is one of the most employed and effective drugs against a wide range of cancers. However, its clinical use for the parenteral administration is accompanied by severe side effects such as high cardiological toxicity and myelosuppression. Therefore, there is a need for development of novel DDSs for DOXO to improve its therapeutic efficacy while minimizing side effects. Ideally, DDSs of DOXO should prevent the release of the drug in plasma and only release it after achieving the tumor site by the enhanced permeability and retention (EPR) effect or active targeting in the tumor cells via endocytosis. The

* Corresponding author.
E-mail address: lgug@intec.unl.edu.ar (L.M. Gugliotta).
[1] These authors contributed equally to this work.

http://dx.doi.org/10.1016/j.eurpolymj.2016.02.022
0014-3057/

noticeable difference between the pH from plasma (pH 7.4) to the tumor microenvironment (pH 6.5) and the lysosomes (pH 4.8–5) can be exploited as an internal trigger to release the drugs from DDSs [9–15]. Engineering nanogels (NGs) could be the key to fulfill the DDSs requirements thanks to their intrinsic properties [16]. NGs are 3D water swellable and dispersable crosslinked polymers that can be prepared in the nanometer range with excellent biocompatibility and softness. These nanomaterials have showed several important advantages over other nano DDSs (e.g., liposomes, micelles, polymersomes), namely, stability, ease of synthesis, good control over particle size, a great variety of functional groups, and easy postsynthetic functionalization [17]. The 3D structure, the nanometric size, the high dispersability in biological fluids, and the possibility of introducing several functional groups enable their utilization as biomaterials for transporting many active pharmaceutical (siRNA, proteins, and drugs) that can be strategically released at cellular levels. The method for NGs synthesis is an important factor when considering the scalable production of DDSs necessary for their translation to the clinic. Thus, compared to other techniques such as inverse miniemulsion polymerization [18] or inverse nanoprecipitation [19], precipitation/dispersion polymerization [20,21] seems to be an easily scalable methodology for preparing NGs without the use of organic solvents nor high ultrasonic energy and with acceptable control over particle size and dispersability. In addition, though precipitation/dispersion polymerization is limited to the preparation of NGs using thermosensitive monomers like NIPA or oligoethyleneglycol methacrylate (OEGMA), the procedure permits incorporation through copolymerization of acceptable amounts of any class of vinyl monomers or vinyl functionalized polymers on the NGs structure, thereby increasing the versatility of the obtained materials [22].

In this work, the synthesis and characterization of different NGs using precipitation/dispersion polymerization based on poly(N-isopropylacrylamide) [poly(NIPA)] and poly(acrylic acid) [poly(AAc)] are presented in detail. While poly(NIPA) based NGs can be easily prepared by precipitation/dispersion polymerization [20,23], the presence of carboxylic groups would allow electrostatic interaction with doxorubicin hydrochloride (DOXO·HCl) and a triggered release under acidic endocytosis pH [24]. Although, NIPA-AAc-based micro/nanogels were studied in detail in the past, their use as DDSs of DOXO·HCl was reported only by few groups [25–29]. Serpe and coworkers [27] reported the thermally regulated uptake and release of DOXO·HCl from microgel thin films built by a layer by layer assembly approach. Zhan et al. [25] developed a system using N,N-bis (acryloyl)cystamine as crosslinker in order to introduce a redox sensitivity to the carrier which enabled drug release by degradability of the carrier in the intracellular reductive conditions. Kumacheva and collaborators [26] reported the potential of the NIPA-AAc NG systems as DOXO·HCl, however they limited they work to the mol% ratio 9:1 between NIPA and AAc. Mao et al. [28] studied cross-linked microgel particles prepared by precipitation polymerization of NIPA, poly(ethylene glycol)diacrylate and AAc. Also, the cell penetrating peptide TAT and a fluorescent probe were immobilized on them. In this case, the influence of temperature change on the cell viability after being incubated with DOXO-loaded microgel particles and free DOXO was investigated. Hydrogel nanocapsules of NIPA-AAc [29] were prepared using hydroxypropylcellulose-poly(AAc) (HPC-AAc) template particles, followed by the surface polymerization of NIPA and the final removal of HPC cores. The yielded capsules were loaded with DOXO·HCl and the release was responsive to the temperature and pH of the media, showing a low-rate but sustained release behavior. Therefore there is still a lack of a systematic study regarding the best NIPA/AAc ratio for an optimal encapsulation and release of DOXO·HCl in cancer cells. Hence, various NG-DOXO·HCl DDSs formulations were prepared and the drug release was evaluated *in vitro*. In this context, the obtained results will give crucial information for further developments of this highly versatile drug-carrier combination. Moreover, the concepts developed in this work could result as a starting point for the development of different NGs with improving technologies such as biodegradability and active targeting to cancer cells.

2. Experimental section

2.1. Materials

The following chemicals were used as purchased: acrylic acid (AAc, Aldrich 98%); N-isopropylacrylamide (NIPA, Aldrich 97%); ammonium persulphate (APS, Aldrich 98%); N,N′-methylenebisacrylamide (BIS, Aldrich 99%); sodium dodecyl sulphate (SDS, Cicarelli); DOXO·HCl (Aldrich); 4-dimethylaminopyridine (DMAP, Aldrich); hydroxybenzotriazole (HOBt, Aldrich), 1-ethyl-3-(3-dimethylaminopropyl)carbodiimide (EDC, Aldrich); cyanine 5 amino (Cy5.0-NH_2, Mivenion); 3-(4,5-dimethylthiazol-2-yl)-2,5-diphenyltetrazolium bromide (MTT); dimethylsulfoxide (DMSO, Across).

2.2. Synthesis of NGs

In a typical procedure for the synthesis of NGs, a certain amount of NIPA, AAc, BIS, SDS, and APS was dissolved in distilled water (20 mL) in a 30 mL flask, hermetically closed with a septum and stirred for 5 min. Then, the mixture was deoxygenated for 5 min with nitrogen and transferred to a hot bath at 70 °C to activate the polymerization process. After 15–20 min of reaction, the solution became cloudy indicating that the polymerization had started. The mixture was stirred at 400 rpm at 70 °C for 4 h. The product was dialyzed for 2 days in 1 L (4 changes of solvent) of distilled water using a dialysis membrane (MWCO 10 kDa) and then lyophilized to obtain cotton like white solid with yields above 80%. NGs with different composition were prepared by a systematic variation of the NIPA/AAc feed-ratio, while maintaining constant the total monomer molar concentration, SDS, and BIS. Accordingly to the feed monomer composition the NGs were named as NIPA 100; NIPA:AAc

(90:10); NIPA:AAc (80:20); NIPA:AAc (70:30), NIPA:AAc (60:40); NIPA:AAc (50:50). Table 1 presents the experimental conditions for the synthesis of the NGs.

Alternatively, Cy5.0-labeled NGs were synthesized for use in cellular uptake studies. Briefly, 20 mg NGs, 0.55 mg of EDC, 0.2 mg DMAP, 0.38 mg HOBT and 0.75 mg Cy5.0-NH_2 were dissolved in 1 mL of phosphate buffer (PB, 10 mM, pH 7.4). The reaction took place in the dark, at room temperature (RT), and stirring overnight. Successfully coupling of the dye was checked by TLC, and the product was purified by size exclusion chromatography (SEC) with Sephadex G25 Fine and then lyophilized.

2.3. Potentiometric titration

The incorporated amount of AAc monomer in the NGs was obtained by titration with 0.01 M of NaOH using an automatic potentiometric titrator KEM AT-510. Thus, 2.5–10 mg (according to AAc amount) of each freeze-dried NG was dispersed into 30 mL of deionized water. NaOH aliquots were added automatically for the titration equipment to the NGs solutions and the pH was measured after each addition. The equivalence point was determined as the maximum of the first derivate of a pH vs. volume of NaOH curve.

2.4. Chemical structure characterization

Water suppression ^{1}H NMR analysis was performed using a Bruker 300 MHz NMR spectrometer at RT. To this effect, 4.5 mg of each NG were dispersed in 0.5 mL of distilled water (H_2O) and 0.15 mL of deuterated water (D_2O) at RT for 24 h prior to the NMR measurement. Fourier Transformed Infrared Spectroscopy (FT-IR) analysis was carried out using a Bruker IFS 66 FT-IR spectrophotometer over the dry NGs.

2.5. Scanning electron microscopy (SEM)

The shape of the re-dispersed (after lyophilization) NG particles was studied by SEM using a Hitachi Scanning Electron Microscope (SU8030). The samples were prepared by deposition of the NGs (0.01 mg mL^{-1}) onto a highly ordered pyrolytic graphite sheet and stained after drying with an aqueous solution of uranyl acetate (1%).

2.6. Atomic force microscopy (AFM)

AFM measurements were recorded by tapping mode with a MultiMode 8 AFM equipped with a Nanoscope V controller from Veeco Instruments, Santa Barbara, California. Data were analyzed using NanoScope Analysis 1.3 software. NG aqueous redispersions (2 mg mL^{-1}) were spin coated on a Mica sheet at 70 rps for 2 min. Samples were analyzed by Nano World tips, Point Probe® Plus Non-Contact / Tapping Mode - Long Cantilever - Reflex Coating (PPP-NCLR20), with resonance frequency of 190 kHz and force constant of 48 N m^{-1}.

2.7. Dynamic light scattering (DLS) and Zeta potential (ZP)

The NGs average particle sizes and the dispersity of the particles size distribution were measured in acetate buffer: pH 4 (50 mM), and 5 (50 mM) and phosphate buffer pH 7.4 (50 mM) at 25 or 37 °C by DLS using a Nano-ZS 90 Malvern equipped with a He–Ne laser (633 nm) under a scattering detection angle of 173°. Samples were prepared by re-dispersion of the NGs (2 mg mL^{-1}) in the above-mentioned buffer solutions of pH 4, 5, and 7.4 one day prior to the experiments. All the samples were maintained for stabilization at the designed temperature for 5 min before testing. Average particle sizes and size distribution are given as the average of 3 measurements. Zeta potential of the NGs was also measured in the same conditions.

2.8. NG-DOXO·HCl formulations

2.8.1. Incorporation of DOXO·HCl into the NG

For these experiments, 20 mg of the NG (NIPA:AAc (80:20), NIPA:AAc (70:30) and NIPA:AAc (60:40)) lyophilized powder were re-dispersed in 4 mL of deionized water and stirred for 15 min. The pH of the dispersion was adjusted to pH = 6.3–6.4 with drops of NaOH 0.1 M. Then, pre-determined amounts of solid DOXO·HCl (for neutralization of 50 or 25% of the acid groups in each NG) were added into the NG dispersion and the mixture was vigorously stirred for 24 h in the dark. The obtained red dispersions were dialyzed against deionized water for 24 h (200 mL, the solvent was changed three times) at RT using a dialysis membrane of 10 kDa (MWCO) in order to eliminate the non-loaded drug. Before each change of deionized water, 1 mL of the dialysis solution was taken. The absorbance of each aliquot was measured at 485 nm to determine the drug loading content (DLC) and drug loading efficiency (DLE) by difference calculated according to the following Eqs. (1) and (2), respectively:

$$\text{DLC (wt\%)} = (\text{weight of loaded drug/weight of drug-loaded NG}) \times 100 \quad (1)$$

Table 1
Experimental conditions for the preparation of NGs at 70 °C.

NGs	NIPA (mol%)	AAc (mol%) feed ratio	AAc (mol%) in the product [a]	Yield (%)
NIPA 100	100	0	0	89.9
NIPA:AAc (90:10)	90	10	9.5	85.2
NIPA:AAc (80:20)	80	20	17.2	89.5
NIPA:AAc (70:30)	70	30	29.3	85.5
NIPA:AAc (60:40)	60	40	34.1	83.5
NIPA:AAc (50:50)	50	50	47.2	95.3

Total monomers concentration (NIPA + AAc) = 0.086 M; BIS = 4% mol respect to monomers; APS = 4% mol respect to monomers; SDS 0.0034 M.
[a] Determined by titration.

$$\text{DLE (wt\%)} = (\text{weight of loaded drug/weight of feeding drug}) \times 100 \quad (2)$$

A calibration curve of DOXO·HCl was performed in deionized water (0.1; 1; 5; 10; 15; 25; 37.5; 50; and 75 μg mL^{-1}) for the determination of DOXO·HCl concentration in the dialysis solutions. The DOXO·HCl loaded-NGs dispersions were freeze-dried in the dark, weighted, and stored for future utilization. As example, the formulations were named as NIPA:AAc (70:30)-DOXO·HCl[25] according to the name of the NG used, followed by DOXO·HCl and followed by the percentage of acid groups of the NG neutralized with DOXO·HCl, in this case 25%. A control experiment of dialysis was realized for free DOXO·HCl in order to be sure that the total of free DOXO·HCl could be eliminated by dialysis. Thus, 17.42 mg of DOXO·HCl (the same amount to prepare the most loaded NGs) was dissolved in 4 mL of deionized water and dialyzed against deionized water (200 mL, three changes of solvent). The amount of DOXO·HCl inside the dialysis bag was determined after finishing the dialysis process, by measuring the absorbance at 485 nm.

2.8.2. In vitro release of DOXO·HCl from the formulations

To determine the drug release of DOXO·HCl from NG-DOXO·HCl formulations, a certain amount (2 mg of NG constant) of the freeze-dried DOXO·HCl-loaded NGs were reconstituted in 1.5 mL of deionized water at 25 °C under stirring for 10 min and then transferred into a circular plastic tube with a membrane of dialysis (MWCO 10 kDa) at the end of the tube held with Teflon. The release experiment was initiated by placing the tube (beyond the level of the donor solution with the release medium) into 30 mL of the release medium, phosphate buffer saline (PBS) pH 7.4 (10 mM buffer, 0.14 M NaCl) for simulation of extracellular plasma release or acetate buffer saline (ABS) pH 5 (10 mM buffer, 0.14 M NaCl) for simulation of intracellular endocytic release, at 37 °C with constant stirring. At selected time intervals, 1 mL of the release medium was taken out and replenished with an equal volume of fresh media maintained at 37 °C. The amount of DOXO·HCl released was determined by UV–vis spectrophotometry measuring the absorbance at 485 nm. A control release experiment was realized with free DOXO·HCl. Calibration curves were realized in ABS pH 5 and PBS pH 7.4 using the following DOXO·HCl concentrations (0.1; 1; 5; 10; 20; 30; 40; and 50 μg mL^{-1}). The experiments of drug release were realized by duplicate.

2.9. Biological assays

2.9.1. Cytotoxicity assay

In vitro toxicity of the NGs was investigated by MTT assay on A549 lung cancer cells (#ACC 107, DSMZ-German collection of Microorganisms and Cell Cultures). Cells were seeded at 10,000 cells/well in 96-well cell culture plates and grown over night in Dulbecco's Modified Eagle Medium (DMEM) with 10% fetal bovine serum (FBS Superior, Millipore), 100 U mL^{-1} penicillin and 100 μg mL^{-1} streptomycin at 37 °C and 5% CO_2. The next day, medium was replaced with 50 μL fresh medium and 50 μL of 2-fold concentrated serial dilutions of the NG samples in triplicates. After 48 h incubation at 37 °C and 5% CO_2, cell culture medium was removed and replaced with 10 μL MTT (0.5 mg mL^{-1} in PBS) in 100 μL fresh medium and incubated another 4 h. Formazan crystals were dissolved in 100 μL/well isopropanol / 40 mM HCl and absorbance was measured at 570 nm. Relative viabilities were calculated by dividing average absorbance values of the samples by values for untreated control cells. Tests were performed at least three times independently.

2.9.2. Cellular uptake - Confocal laser scanning microscopy (cLSM)

Cellular uptake of DOXO·HCl loaded NIPA:AAc (80:20) NGs or Cy5.0-labeled NIPA:AAc (80:20) was monitored by confocal microscopy. 100,000 A549 cells mL^{-1} were seeded on coverslips in 24-well plates and allowed to adhere overnight. For expression of fluorescent lysosome marker protein GFP-LAMP-1, cells were transfected with CellLight® Lysosomes-GFP, BacMam 2.0 (Invitrogen) according to the manufacturer's protocol.

After overnight incubation, a dispersion of DOXO·HCl loaded or Cy5.0-labeled NIPA:AAc (80:20) NG were added and incubated for 1–24 h at 37 °C. After incubation with the NGs, cells were washed 3 times with PBS and fixed with 10% neutral buffered formalin for 20 min. After 3 washing steps with PBS, cell nuclei were stained with 4′,6-diamidino-2-phenylindole (DAPI, 2.5 μg mL^{-1} in PBS) for 30 min. Slides were washed again, mounted on microscope slides using ProTaqs MountFluor (Quartett GmbH, Germany) and dried overnight. Images were acquired using a Leica SP8 confocal laser scanning microscope

and LASAF software (DAPI: Ex. 405 nm, Em. 380–385 nm, GFP: Ex. 488 nm, Em. 500–550 nm; DOXO: Ex. 496 nm, Em. 530–749 nm, Cy5.0: Ex. 633 nm, Em. 641–769 nm).

2.9.3. In vitro cancer cell growth inhibition

The *in vitro* cancer cell growth inhibition was studied by MTT following the same procedure described above in Section 2.9.1. Different concentrations of NIPA:AAc (80:20)-DOXO·HCl[25] ranging from 0.0001 to 10 μM based on DOXO·HCl were tested and compared with the same concentrations of free DOXO·HCl.

3. Results and discussion

3.1. Synthesis and chemical characterization of the NGs

The synthesis of NGs based on NIPA and AAc was carried out by the radical precipitation/dispersion polymerization technique schematized in Fig. 1. The reaction temperature is above the LCST of NIPA and, consequently, after achieving a critical molecular weight, the growing polymers were separated from the homogeneous phase generating particles that were stabilized by the surfactant to prevent decantation. It was visible due to the presence of turbidity in the previous transparent homogeneous solution.

The incorporation of AAc into the NG networks was made by copolymerization of AAc with NIPA in different molar ratios. A systematic variation of the NIPA/AAc monomer feed ratio up to 50% of AAc (Table 1) was realized in order to introduce acid functionality over the NIPA based NGs structures. It should be noted that the addition of high amounts of AAc could prevent or retard the precipitation process and drastically increase the size and size dispersity of the obtained NGs, which is not desirable. All the prepared NGs were obtained as white, cotton like products in very good yields of 85–95% after exhaustive dialysis and lyophilization. The final percentages of AAc incorporated to the NGs were determined by potentiometric titration (see Fig. S3 in SI) and resulted very close to the initial feed ratio for all the prepared NGs as shown in Table 1. An acceptable amount of AAc (up to 34.1% in mol) could be incorporated in the NGs structures without losing the particle size and dispersity control as shown by DLS (Table 2). On the other hand, high polydispersity index (PDI) was observed for higher AAc contents like NIPA:AAc (50:50). Note that, a high incorporation of AAc is important in order to obtain NGs with major acid functionality and therefore to increase the loading of DOXO·HCl by ionic interaction.

Chemical composition of the NGs was also supported by ^{1}H NMR and FT-IR (Figs. S1 and S2 in SI). In the NMR spectra of the NGs, a decreasing change is clearly observed in the signals at 3.76 and 7.69 ppm (corresponding to C**H**$(CH_3)_2$ and N**H** of NIPA, respectively) with respect to the polymer backbone signals (—C**H**C**H**$_2$—) between 1.2 and 2.2 ppm from NIPA 100 to NIPA:AAc (50:50). In addition, an increment in the signal at 2.62 ppm, corresponding to the O**H** of AAc, was observed from NIPA 100 to NIPA:AAc (50:50). FT-IR spectra showed a relative increment in the signal at 1710 cm^{-1} corresponding to the carbonyl groups (C═O) of AAc and a relative diminution in the signal of band I at 1639 cm^{-1} and II at 1538 cm^{-1} of amide (NIPA signals) from NIPA:AAc (90:10) to NIPA:AAc (50:50).

3.2. Physicochemical characterizations of the NGs

3.2.1. SEM and AFM microscopy

SEM and AFM images show that the NGs presented quite spherical 3D morphology and acceptable narrow size distribution. As an example, NIPA:AAc (80:20) images are shown in Fig. 2. The size of the NG NIPA:AAc (80:20) is around 60 nm as determined by SEM image (Fig. 2a) and 130 nm by AFM image (Fig. 2b). The observed difference in size rely in the measurement conditions of both techniques; while SEM is measure in dry vacuum, AFM is measured in ambient conditions where the NGs are slightly swollen.

3.2.2. Dynamic light scattering (DLS)

The hydrodynamic average diameter and PDI of NIPA:AAc based NGs were measured under different conditions of pH and temperature. Thus, the size of the NGs at pH 4, and relevant physiological pH, pH 5 (inside of the endosomes) and 7.4 (plasma) at 25 or 37 °C were measured. The results are shown in Table 2. Regarding the potential biomedical applications of these nanomaterials as carriers for DDSs of anticancer drugs to cellular levels, the NGs NIPA:AAc (90:10), (80:20), (70:30), and (60:40) showed very good dispersability and presented average sizes from 207 to 275 nm at simulated plasma conditions (pH 7.4 and 37 °C) and 125–261 nm at simulated endosomal conditions (pH 5 and 37 °C). According to previous studies [30], nanoparticles with sizes between 10 and 200 nm could elude more easily the reticuloendothelial system (RES) therefore avoiding systemic elimination after injection and increasing the systemic circulation. The NG NIPA 100 precipitated at pH 7.4 or 5 at 37 °C and it is consequently not interesting for utilization as carrier for systemic applications. In addition, NIPA:AAc (50:50) showed a size of 553 and 389 nm with high PDI at both pH 7.4 and 5, respectively, at 37 °C, and, for this reason, it was also discarded for future application in drug delivery. Except for NIPA 100, no significant difference in the size of the NGs at pH 7.4 and 5 at both temperatures 25 and 37 °C was observed suggesting that the total ionization of the acid groups of the poly(AAc) segments (pKa = 4.35) was the driving force of the network expansion against the collapsed force imposed for poly(NIPA) segment above its LCST, 32 °C. At simulated conditions of lysosome internalization, pH 5

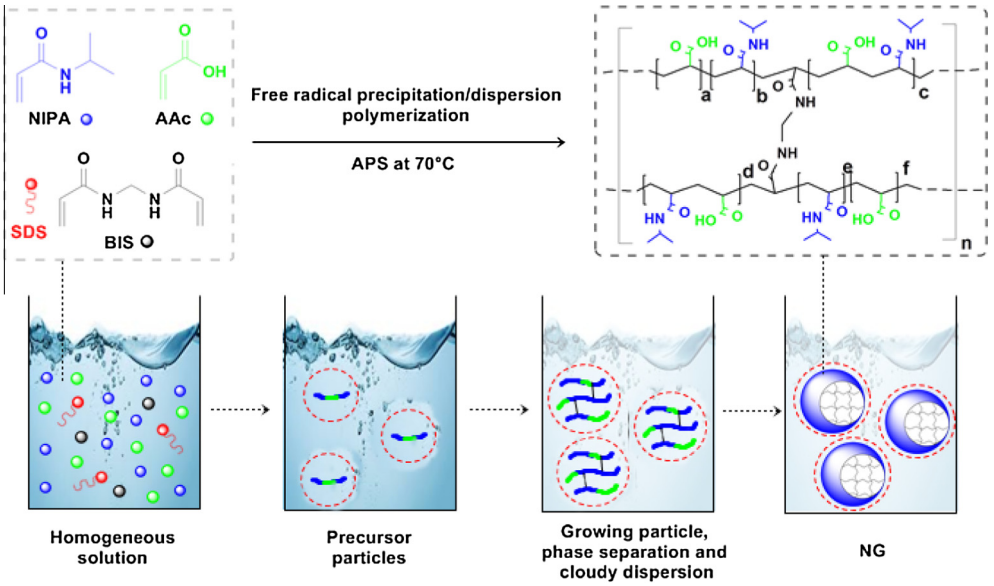

Fig. 1. Synthesis of NGs by free radical precipitation/dispersion polymerization using BIS as crosslinker, APS as initiator, and SDS as stabilizer.

Table 2
Size of the NGs under different conditions measured by DLS.

NG	Size (nm) (PDI)					
	25 °C			37 °C		
	pH 4	pH 5	pH 7.4	pH 4	pH 5	pH 7.4
NIPA 100	114.0 (0.158)	110.6 (0.131)	108.8 (0.119)	[a]	[a]	[a]
NIPA:AAc (90:10)	114.3 (0.180)	131.1 (0.198)	197.9 (0.179)	74.7 (0.053)	124.5 (0.169)	206.7 (0.177)
NIPA:AAc (80:20)	147.1 (0.136)	176.4 (0.168)	210.0 (0.201)	113.5 (0.164)	179.7 (0.160)	221.2 (0.257)
NIPA:AAc (70:30)	187.2 (0.177)	226.6 (0.200)	242.0 (0.210)	127.0 (0.137)	233.3 (0.187)	254.2 (0.196)
NIPA:AAc (60:40)	201.3 (0.152)	246.1 (0.180)	259.9 (0.199)	165.7 (0.124)	260.5 (0.180)	274.9 (0.191)
NIPA:AAc (50:50)	337 (0.295)	370 (0.394)	414 (0.657)	329 (0.251)	389 (0.344)	553 (0.621)

[a] Precipitation was observed. All buffers were 50 mM; pH 4 and 5, buffer acetate; pH 7.4 buffer phosphate.

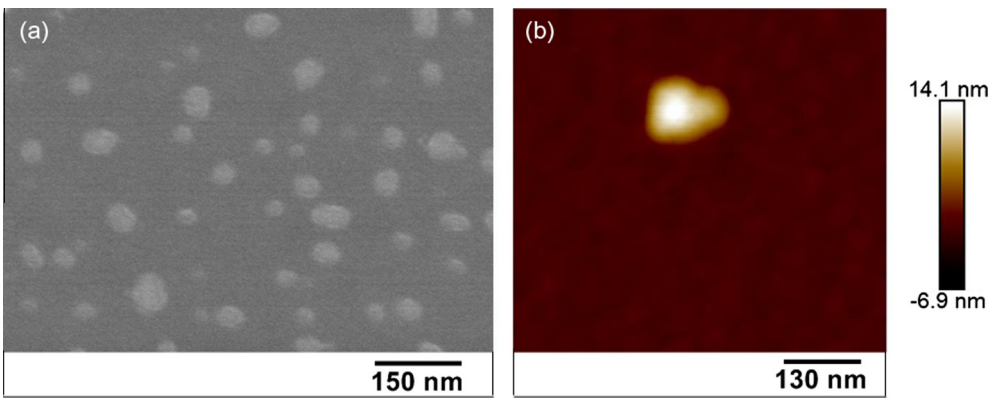

Fig. 2. (a) SEM and (b) AFM images of NG NIPA:AAc (80:20).

and 37 °C, the four selected NGs, NIPA:AAc (90:10), (80:20), (70:30) and (60:40), maintained the dispersability (no visible turbidity was observed) with a small decrease in their sizes which was less noticeable when major amount of AAc was present in the network compared to pH 7.4 at 37 °C. This small decrease in the size was due to the partial protonation of acid groups of poly(AAc) segments at pH 5, which generated a less expanded network. The decrease on size from pH 7.4 to 5 is almost undetectable for the NGs NIPA:AAc (80:20), (70:30) and (60:40). Identical to the size of the NGs at pH 7.4 at 25 or 37 °C, no difference in the size of NGs at pH 5 at 25 or 37 °C was observed. Finally, though it is not relevant for bioapplications but could possibly support the protonation-collapse theory, slight turbidity and a smaller size were observed for NIPA:AAc (90:10), (80:20) and (70:30) at pH 4 at 37 °C. In this case, almost all NGs acid groups are protonated at pH 4, and therefore avoided network expansion for ionization. Consequently the networks could be more easily collapsed in response to the negative temperature dependence swellability of the poly(NIPA) segments.

The zeta potential of all AAc-containing NGs was negative at all studied pHs (pH 4; 5; and 7.4, see Table S1 in SI). The zeta potential of NGs decreased with the pH from pH 4 to pH 7.4 according to the amount of ionized carboxylic groups at each particular pH.

3.3. NGs-DOXO·HCl formulations

3.3.1. Preparation and characterization of the formulations

Based on NG characterization, especially in the size and good dispersability at pH 5 and 7.4 at 37 °C and acceptable amount of AAc, the three most promising NGs [NIPA:AAc (60:40); NIPA:AAc (70:30) and NIPA:AAc (80:20)] were used for the preparation of new NG-DOXO·HCl DDSs. Different DOXO·HCl formulations using the NGs as carrier were prepared by simple mixing the NG and DOXO·HCl in aqueous solution at pH 6.2. At this pH, NIPA:AAc based NGs presented negative charge (pKa of poly(AAc) = 4.35) while DOXO·HCl exhibited positive charge (pKa DOXO-NH_3^+ = 8.3) resulting in the formation of an efficient ionic interaction system between the polymer and the drug, as it is shown in Fig. 3.

Evidence of a strong interaction between DOXO·HCl and anionic NGs was demonstrated by UV–Vis comparing the spectrum of free DOXO·HCl with the spectrum of the mixture NGs-DOXO·HCl at the same DOXO·HCl concentration (see Fig. S4 in SI). Diminution of the absorbance and a bathochromic effect ware clearly observed when DOXO·HCl was in presence of the NG NIPA:AAc (70:30), suggesting a strong interaction of the drug with the polymer. Six formulations were prepared and their properties are presented in Table 3. The superscript 25 or 50 in the name of the formulations, indicates that a total of 25 or 50 mol% of acid groups were neutralized with DOXO·HCl. Drug loading efficiency (DLE) for the NGs was excellent (above of 90%) for all the prepared formulations as determined after non-drug loaded elimination by dialysis. In addition, good to excellent drug loading content (DLC) from 15.9 to 45.8%, were obtained depending on the amounts of DOXO·HCl added in the preparation of the formulations. All the formulations prepared with 25% of acid neutralization [NIPA:AAc (80:20)-DOXO·HCl^{25}; NIPA:AAc (70:30)-DOXO·HCl^{25}; NIPA:AAc (60:40)-DOXO·HCl^{25}] were able to be quickly re-disperse after lyophilization which is highly desirable for a possible future parenteral administration. On the other hand, though it was possible to load greater amounts of DOXO·HCl with 50% of NG acid neutralization for the three NGs, these formulations [NIPA:AAc (80:20)-DOXO·HCl^{50}; NIPA:AAc (70:30)-DOXO·HCl^{50}; NIPA:AAc (60:40)-DOXO·HCl^{50}] presented serious problems for the total re-dispersion after lyophilization and consequently they were discarded for potential applications.

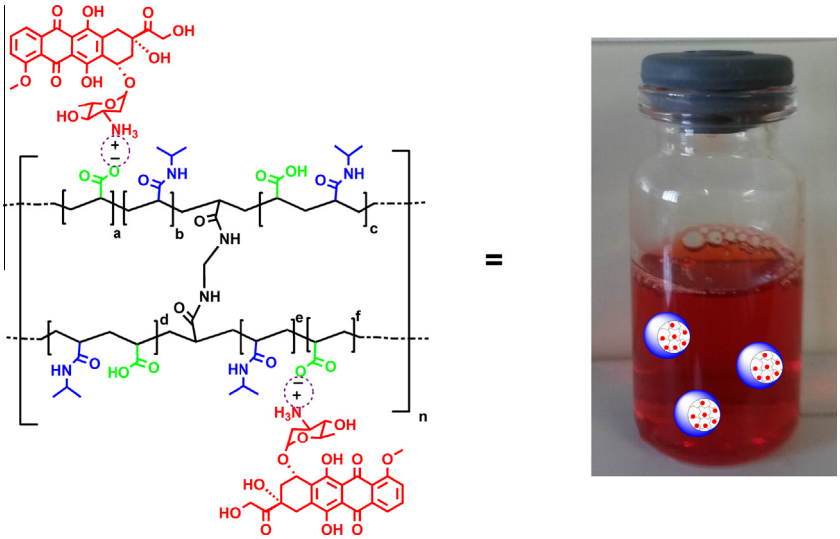

Fig. 3. Schematic representation of the ionic NG-DOXO·HCl formulations. Photo: NIPA:AAc (80:20)-DOXO·HCl^{25}. The superscript 25 in the name of the formulations indicate that a total of 25% in mol of acid groups present in the NG structure were neutralized with DOXO·HCl.

Table 3
Properties of the prepared NG-DOXO·HCl formulations.

Formulations	DLC (%)	DLE (%)	Precipitation after 24 h of loading	Dispersibility after lyophilization
NIPA:AAc (80:20)-DOXO HCl^{25}	15.9	90.6	No	Yes
NIPA:AAc (80:20)-DOXO HCl^{50}	27.7	91.9	No	No
NIPA:AAc (70:30)-DOXO HCl^{25}	24.4	87.8	No	Yes
NIPA:AAc (70:30)-DOXO HCl^{50}	40.6	93.0	No	No
NIPA:AAc (60:40)-DOXO HCl^{25}	29.8	97.4	No	Yes
NIPA:AAc (60:40)-DOXO HCl^{50}	45.8	97.2	No	No

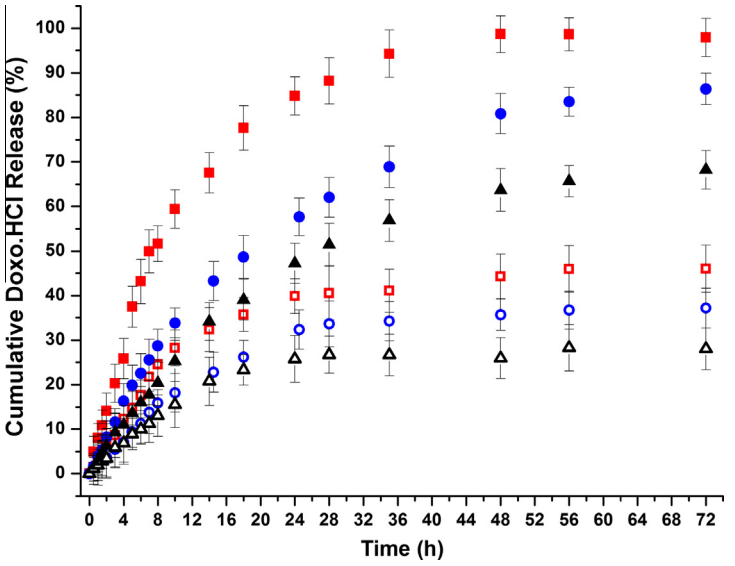

Fig. 4. Release profiles from NG-DOXO·HCl formulations at 37 °C under constant ionic force (0.14 M NaCl) and different pH conditions: NIPA:AAc(80:20)-DOXO·HCl^{25} at pH 5 (■) and 7.4 (□); NIPA:AAc(70:30)-DOXO·HCl^{25} at pH 5 (●) and 7.4 (○); NIPA:AAc(60:40)-DOXO·HCl^{25} at pH 5 (▲) and 7.4 (△).

3.3.2. In vitro release studies

In order to study the release behavior of the different formulations, various *in vitro* release experiments were carried out in physiological and lysosomal conditions. Fig. 4 shows the *in vitro* DOXO·HCl release profiles from the formulation: NIPA:AAc (80:20)-DOXO·HCl^{25}, NIPA:AAc (70:30)-DOXO·HCl^{25}, and NIPA:AAc (60:40)-DOXO·HCl^{25} in physiological [phosphate buffer pH 7.4 (10 mM) + NaCl 0.14 M] and lysosomal [acetate buffer pH 5 (10 mM) + NaCl 0.14 M] simulated media at 37 °C.

It can be seen that, at any time, all formulations released major percentage of DOXO·HCl release at pH 5 compared with pH 7.4. For example, the formulation NIPA:AAc(80:20)-DOXO·HCl^{25} released 84 and 39% of DOXO·HCl at pH 5 and 7.4, respectively. Possibly, at pH 5, most of the carboxylic groups in the NG (from poly(AAc) with pKa = 4.3) could be newly protonated, disrupting consequently the NG-DOXO ionic interaction of the formulations and increasing the DOXO·HCl release. On the other hand, there is not a favorable breaking of the NG-DOXO·HCl ionic interaction at pH 7.4 (almost neutral pH) and consequently a minimal DOXO·HCl release is observed.

In addition, the diffusion of free DOXO·HCl trough the dialysis membrane (using the same amount of DOXO loaded in NIPA:AAc(80:20)-DOXO·HCl^{25}) at pH 5 or 7.4 (see Fig. S5 in SI)) were very similar between them and also between the release profile of NIPA:AAc(80:20)-DOXO·HCl^{25} at pH 5. This result, suggests that the NG participates actively controlling the release profiles with minimal release at pH 7.4 and high release at pH 5. At this last pH, a rapid NG-DOXO ionic dissociation appears immediately upon contact with the pH release medium, activating the fast release of the drug.

The increased release of DOXO·HCl from this novel NG-DOXO·HCl formulations from pH 7.4 to 5 shows great potential for cancer therapies based on the antiproliferative effect. These formulations could present less adverse effects of cancer drugs after parenteral administration because of the release of DOXO·HCl inside the cells (pH 5) while limiting its release in blood circulation (pH 7.4). In addition the formulations could be accumulated in tumor sites by the known EPR effect and release the drug only in tumor cells after cell internalization.

3.4. Biological characterizations of NGs

3.4.1. Intrinsic toxicity

The promising physicochemical properties of these carriers encourage us to perform the biological characterization in order to use them in biomedical applications. The cytotoxicity of NGs was evaluated in A549 tumor cells by the MTT assay.

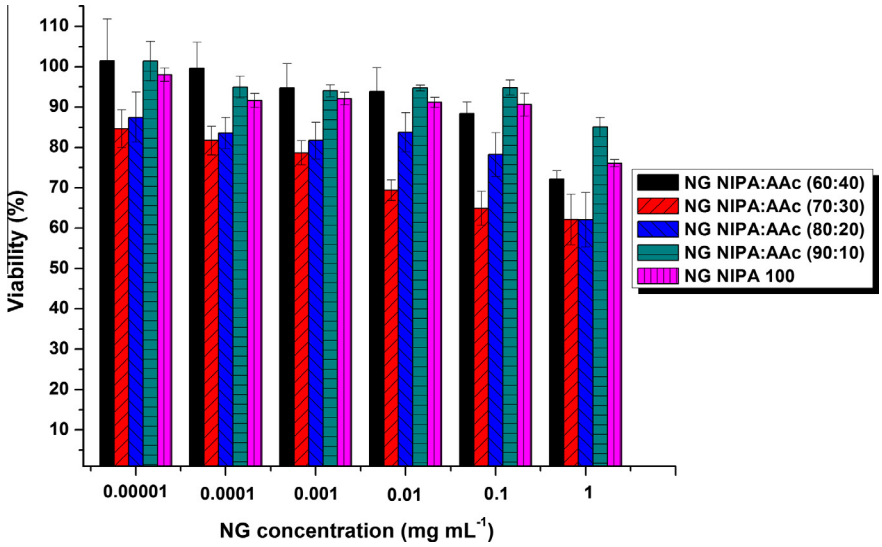

Fig. 5. Intrinsic toxicity of NGs determined by the MTT assay.

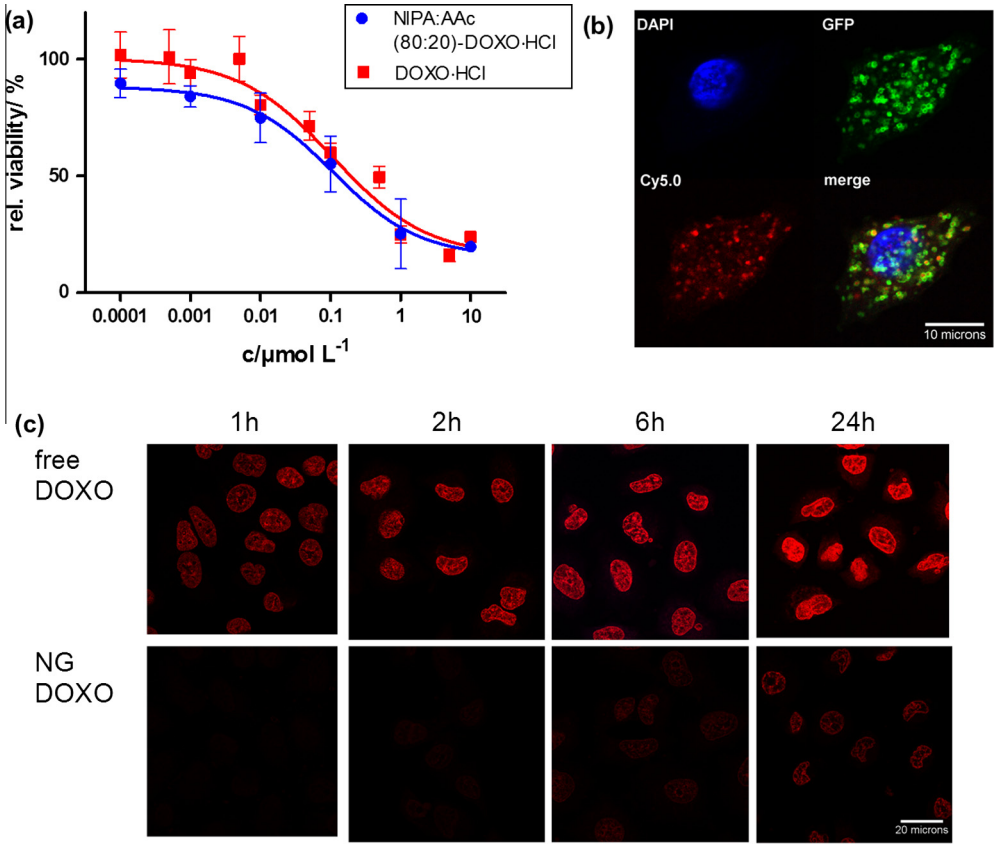

Fig. 6. (a) Toxicity of the formulation NIPA:AAc(80:20)-DOXO·HCl[25] on A549 cancer cells determined by MTT test. (b) Cellular localization of Cy5.0-labeled NIPA:AAc(80:20) NG, blue: DAPI stained cell nuclei, green: lysosome marker LAMP-1-GFP, red: Cy5.0 labeled NG. (c) Delivery of DOXO to the cell nuclei from NIPA:AAc(80:20)-DOXO-HCl[25] compared with the same concentration of free DOXO after 1, 2, 6, and 24 h of incubation. (For interpretation of the references to color in this figure legend, the reader is referred to the web version of this article.)

As it can be seen in Fig. 5, a viability of more than 60% was observed in the MTT assay after 48 h of treatment for all NGs, demonstrating a good cytocompatibility of the synthesized carriers up to a concentration of 1 mg mL^{-1}.

3.4.2. Tumor cell growth inhibition

Since the use of these carriers was proposed for anticancer therapy, the performance of the DOXO·HCl-loaded NGs compared with free DOXO·HCl in A549 tumor cells was studied. NIPA:AAc(80:20)-DOXO·HCl[25] was chosen to carry out the experiment of tumor cell growth inhibition because it shown the best release profile of DOXO·HCl combined with high biocompatibility.

The dose - response relationship, determined by MTT test, of both NIPA:AAc(80:20)-DOXO·HCl[25] and free DOXO·HCl on A549 cells after 48 h of exposure, was similar (Fig. 6a) with a half-maximal inhibitory concentration (IC50) of about 0.1 μM for both. Comparing with the release profiles in Fig. 6, it seems plausible that the NGs have passed acidic conditions in the (intracellular) environment, enabling all DOXO·HCl to be released and to inhibit cell growth after 48 h. This intracellular pathway was also supported by the cellular uptake experiments shown in Fig. 6b, where it can be seen that Cy5.0-labeled NIPA:AAc(80:20) is mainly localized within compartments labeled with a fluorescent lysosome marker protein (GFP-LAMP-1). Additionally, in order to prove that the drug is not being release outside the cell, the kinetics of DOXO·HCl delivery to the cell nuclei was monitored over time and compared to free DOXO·HCl (Fig. 6c).

The images after selected incubation times (1, 2, 6, and 24 h) shown in Fig. 6c confirm that in contrast to free DOXO, which is quickly accumulated in the nuclei in 1 h already, the same concentration of DOXO needs over 24 h to accumulate when it was encapsulated within the NG. This desirable feature would greatly reduce side effects caused by passive diffusion and uptake of the free drug before the carrier reaches the target cells.

4. Conclusions

NIPA-co-AAc NGs with different NIPA/AAc molar composition have been designed as carriers of DOXO·HCl for cancer therapies. The NGs showed excellent properties for their further use *in vivo*, as good dispersability in simulated physiological environment, low cytotoxicity, and excellent cellular penetration properties. Moreover, the NGs exhibited high DOXO·HCl loading capacity and efficiency due to the ionic interaction. The formulations showed minimal leakage of the cargo at plasma simulated medium and a triggered sustained release of DOXO·HCl at lysosomal conditions. As the formulation showed the same IC50 of the free drug after 48 h of incubation, no drug activity is lost due to the encapsulation within the carriers, because the whole cargo can be released at low pH, making these NGs great candidates for application as carriers in cancer therapies. In comparison with previous works [25–29], the effect of NIPA/AAc composition on the behavior of the NGs to be used al DDS of DOXO·HCl was here considered.

Acknowledgements

The authors gratefully thank ANPCyT, CONICET, UNL, and UNC for financial support. Dr. Julio Cuggino also acknowledges the postdoctoral fellowships from CONICET and Garrahan Hospital for DOXO·HCl donation. Dr. M. Calderón gratefully acknowledges financial support from the Bundesministerium für Bildung und Forschung (BMBF) through the NanoMatFutur award (13N12561), the Helmholtz Virtual Institute, Multifunctional Biomaterials for Medicine, and the Freie Universität Focus Area Nanoscale. Dr. Maria Molina acknowledges financial support from the Alexander von Humboldt Foundation.

Appendix A. Supplementary material

Supplementary data associated with this article can be found, in the online version, at http://dx.doi.org/10.1016/j.eurpolymj.2016.02.022.

References

[1] R. Gref, A. Domb, P. Quellec, T. Blunk, R.H. Müller, J.M. Verbavatz, et al, The controlled intravenous delivery of drugs using PEG-coated sterically stabilized nanospheres, Adv. Drug Delivery Rev. 64 (Supplement(0)) (2012) 316–326.
[2] J.K. Oh, R. Drumright, D.J. Siegwart, K. Matyjaszewski, The development of microgels/nanogels for drug delivery applications, Prog. Polym. Sci. 33 (4) (2008) 448–477.
[3] R.T. Chacko, J. Ventura, J. Zhuang, S. Thayumanavan, Polymer nanogels: a versatile nanoscopic drug delivery platform, Adv. Drug Delivery Rev. 64 (9) (2012) 836–851.
[4] M. Elsabahy, K.L. Wooley, Design of polymeric nanoparticles for biomedical delivery applications, Chem. Soc. Rev. 41 (7) (2012) 2545–2561.
[5] M.E. Davis, Z. Chen, D.M. Shin, Nanoparticle therapeutics: an emerging treatment modality for cancer, Nat. Rev. Drug Discovery 7 (9) (2008) 771–782.
[6] M. Witting, M. Molina, K. Obst, R. Plank, K.M. Eckl, H.C. Hennies, et al, Thermosensitive dendritic polyglycerol-based nanogels for cutaneous delivery of biomacromolecules, Nanomedicine 11 (5) (2015) 1179–1187.
[7] E.S. Lee, Z. Gao, Y.H. Bae, Recent progress in tumor pH targeting nanotechnology, J. Controlled Release 132 (3) (2008) 164–170.
[8] N. Bertrand, J. Wu, X. Xu, N. Kamaly, O.C. Farokhzad, Cancer nanotechnology: the impact of passive and active targeting in the era of modern cancer biology, Adv. Drug Delivery Rev. 66 (0) (2014) 2–25.
[9] M. Li, W. Song, Z. Tang, S. Lv, L. Lin, H. Sun, et al, Nanoscaled poly(l-glutamic acid)/doxorubicin-amphiphile complex as pH-responsive drug delivery system for effective treatment of nonsmall cell lung cancer, ACS Appl. Mater. Interfaces 5 (5) (2013) 1781–1792.

[10] J.O. Kim, A.V. Kabanov, T.K. Bronich, Polymer micelles with cross-linked polyanion core for delivery of a cationic drug doxorubicin, J. Controlled Release 138 (3) (2009) 197–204.
[11] J. Ding, W. Xu, Y. Zhang, D. Sun, C. Xiao, D. Liu, et al, Self-reinforced endocytoses of smart polypeptide nanogels for "on-demand" drug delivery, J. Controlled Release 172 (2) (2013) 444–455.
[12] F. Shi, J. Ding, C. Xiao, X. Zhuang, C. He, L. Chen, et al, Intracellular microenvironment responsive PEGylated polypeptide nanogels with ionizable cores for efficient doxorubicin loading and triggered release, J. Mater. Chem. 22 (28) (2012) 14168–14179.
[13] J. Peng, T. Qi, J. Liao, B. Chu, Q. Yang, W. Li, et al, Controlled release of cisplatin from pH-thermal dual responsive nanogels, Biomaterials 34 (34) (2013) 8726–8740.
[14] J. Chen, J. Ouyang, J. Kong, W. Zhong, M.M. Xing, Photo-cross-linked and pH-sensitive biodegradable micelles for doxorubicin delivery, ACS Appl. Mater. Interfaces 5 (8) (2013) 3108–3117.
[15] H.-C. Wang, Y. Zhang, C.M. Possanza, S.C. Zimmerman, J. Cheng, J.S. Moore, et al, Trigger chemistries for better industrial formulations, ACS Appl. Mater. Interfaces 7 (12) (2015) 6369–6382.
[16] A.V. Kabanov, S.V. Vinogradov, Nanogels as pharmaceutical carriers: finite networks of infinite capabilities, Angew. Chem., Int. Ed. 48 (30) (2009) 5418–5429.
[17] M. Molina, M. Asadian-Birjand, J. Balach, J. Bergueiro, E. Miceli, M. Calderon, Stimuli-responsive nanogel composites and their application in nanomedicine, Chem. Soc. Rev. 44 (2015) 6161–6186.
[18] D. Klinger, E.M. Aschenbrenner, C.K. Weiss, K. Landfester, Enzymatically degradable nanogels by inverse miniemulsion copolymerization of acrylamide with dextran methacrylates as crosslinkers, Polym. Chem. 3 (1) (2012) 204–216.
[19] D. Steinhilber, M. Witting, X. Zhang, M. Staegemann, F. Paulus, W. Friess, et al, Surfactant free preparation of biodegradable dendritic polyglycerol nanogels by inverse nanoprecipitation for encapsulation and release of pharmaceutical biomacromolecules, J. Controlled Release 169 (3) (2013) 289–295.
[20] J.C. Cuggino, I.C.I. Alvarez, M.C. Strumia, P. Welker, K. Licha, D. Steinhilber, et al, Thermosensitive nanogels based on dendritic polyglycerol and N-isopropylacrylamide for biomedical applications, Soft Matter 7 (23) (2011) 11259–11266.
[21] M. Asadian-Birjand, J. Bergueiro, F. Rancan, J.C. Cuggino, R.C. Mutihac, K. Achazi, et al, Engineering thermoresponsive polyether-based nanogels for temperature dependent skin penetration, Polym. Chem. 6 (2015) 5827–5831.
[22] M. Molina, M. Giulbudagian, M. Calderón, Positively charged thermoresponsive nanogels for anticancer drug delivery, Macromol. Chem. Phys. 215 (24) (2014) 2414–2419.
[23] Y. Chen, X. Zheng, X. Wang, C. Wang, Y. Ding, X. Jiang, Near-infrared emitting gold cluster–poly(acrylic acid) hybrid nanogels, ACS Macro Lett. 3 (1) (2013) 74–76.
[24] Y. Chen, X. Zheng, H. Qian, Z. Mao, D. Ding, X. Jiang, Hollow core–porous shell structure poly(acrylic acid) nanogels with a superhigh capacity of drug loading, ACS Appl. Mater. Interfaces 2 (12) (2010) 3532–3538.
[25] Y. Zhan, M. Goncalves, P. Yi, D. Capelo, Y. Zhang, J. Rodrigues, et al, Thermo/redox/pH-triple sensitive poly(N-isopropylacrylamide-co-acrylic acid) nanogels for anticancer drug delivery, J. Mater. Chem. B 3 (20) (2015) 4221–4230.
[26] M. Das, S. Mardyani, W.C.W. Chan, E. Kumacheva, Biofunctionalized pH-responsive microgels for cancer cell targeting: rational design, Adv. Mater. 18 (1) (2006) 80–83.
[27] M.J. Serpe, K.A. Yarmey, C.M. Nolan, L.A. Lyon, Doxorubicin uptake and release from microgel thin films, Biomacromolecules 6 (1) (2005) 408–413.
[28] W. Zhang, Z. Mao, C. Gao, Preparation of TAT peptide-modified poly(N-isopropylacrylamide) microgel particles and their cellular uptake, intracellular distribution, and influence on cytoviability in response to temperature change, J. Colloid Interface Sci. 434 (2014) 122–129.
[29] J. Nan, Y. Chen, R. Li, J. Wang, M. Liu, Wang, F. Chu, Polymeric hydrogel nanocapsules: a thermo and pH dual-responsive carrier for sustained drug release, Nano-Micro Lett. 6 (3) (2014) 200–208.
[30] A.H. Faraji, P. Wipf, Nanoparticles in cellular drug delivery, Bioorg. Med. Chem. 17 (8) (2009) 2950–2962.